PAPER

Study of the electrical parameters degradation of GaAs sub-cells for triple junction space solar cells by computer simulation

To cite this article: M A Cappelletti *et al* 2016 *Semicond. Sci. Technol.* **31** 115020

IOP Publishing Semiconductor Science and Technology
Semicond. Sci. Technol. 31 (2016) 115020 (8pp) doi:10.1088/0268-1242/31/11/115020

Study of the electrical parameters degradation of GaAs sub-cells for triple junction space solar cells by computer simulation

M A Cappelletti[1,2], G A Casas[1,3], D M Morales[2], W Hasperue[2,4] and E L Peltzer y Blancá[1]

[1] Grupo de Estudio de Materiales y Dispositivos Electrónicos (GEMyDE), Dpto. de Electrotecnia, Facultad de Ingeniería, Universidad Nacional de La Plata, CONICET, 48 y 116, CC.91, La Plata (1900), Argentina
[2] Universidad Nacional Arturo Jauretche, Avenida Calchaquí 6200, Florencio Varela (1888), Buenos Aires, Argentina
[3] Universidad Nacional de Quilmes, Roque Saenz Peña 352, Bernal (1876), Buenos Aires, Argentina
[4] Instituto de Investigación en Informática LIDI (III-LIDI), Facultad de Informática, Universidad Nacional de La Plata, 50 y 120, La Plata (1900), Argentina

E-mail: marcelo.cappelletti@ing.unlp.edu.ar

Received 27 December 2015, revised 16 August 2016
Accepted for publication 15 September 2016
Published 17 October 2016

Abstract

In this paper, a theoretical study of the electrical parameters degradation of different n-type GaAs sub-cells for InGaP/GaAs/Ge triple junction solar cells irradiated with 1 and 5 MeV electrons has been performed by means of computer simulation. Effects of base carrier concentration upon the maximum power point, short-circuit current, open circuit voltage, diffusion current, recombination current and series resistance of these devices have been researched using the displacement damage dose method, the one-dimensional PC1D device modeling program and a home-made numerical code based on genetic algorithms. The radiative recombination lifetime, damage constant for minority-carrier lifetime and carrier removal rate models for GaAs sub-cells have been used in the simulations. An analytical model has been proposed, which is useful to describe the radiation-induced degradation of diffusion current, recombination current and series resistance. Results obtained in this work can be used to predict the radiation resistance of solar cells over a wide range of energies.

Keywords: GaAs solar cell, space radiation, genetic algorithms, displacement damage dose

1. Introduction

The study of solar cells which can convert solar energy directly into electrical power is becoming increasingly significant, taking into account the urgent need for developing cost-effective alternative energy sources. In the last few years, solar cells have been used in space missions as the main power source for satellites. The space radiation environment is composed of different types of particles over a wide energy range, such as electrons, protons, neutrons, gamma rays, heavy ions, which degrade the performance of the devices. Therefore, the reliability of solar cells in a radiation environment is currently a very important research topic for accurate predictions of the end-of-life (EOL) performance degradation and the on-orbit expected mission lifetime [1–3].

The displacement damage dose (D_d) method and the equivalent fluence method are two main approaches developed at the US Naval Research Laboratory (NRL) and at the US Jet Propulsion Laboratory (JPL), respectively, in order to predict the degradation of a solar cell in the space radiation environment and to mitigate the radiation effects. Both methods include damage by electrons and protons of any energy. On the one hand, the equivalent fluence method is based on the concept of the relative damage coefficient [4],

which is derived from a ground-based experiment with different monoenergetic electron and proton irradiation, usually four electron and eight proton energies [5]. Therefore, a large data set is required from which the energy dependence of the solar cell degradation is empirically determined. On the other hand, in the D_d approach, the energy dependence of the damage coefficients is determined from the calculation of the non-ionizing energy loss (NIEL), which is referred to the rate of energy loss caused by atomic displacements when electrons or protons traverse a certain material [6]. Thus, the solar cell response can be described with limited experimental data (usually two electron and only one proton energies). As a result, in this method, the measured data collapse to a single curve from which the solar cell performance in any energy can be predicted.

Solar cells used in a space environment are expected to respond differently to the radiation effects according to the particular mission variables such as orbital altitude, inclination and elapsed time after launch [7], and to the material, structure and resistivity of the devices [8]. In recent years, multijunction solar cells (MJSC) based on III–V compound semiconductors, particularly InGaP/GaAs/Ge triple junction (3J), have demonstrated higher beginning-of-life (BOL) performance and better radiation resistance compared to Si single crystalline and GaAs devices [9]. In the InGaP/GaAs/Ge 3J solar cell, the top InGaP and the bottom Ge sub-cells are subjected, at a lesser degree, to radiation degradation and consequently the radiation resistance is limited by the middle GaAs sub-cell [10, 11]. Therefore, further research in optimizing the design for GaAs sub-cells is still required to improve the radiation resistance of MJSC.

In this work, the radiation response of twenty different n-type GaAs sub-cells for InGaP/GaAs/Ge 3J solar cells irradiated with 1 and 5 MeV electron energies has been analyzed by means of computer simulation. Mathematical models of radiative recombination lifetime, damage constant for minority-carrier lifetime and carrier removal rate for GaAs sub-cells have been used in the simulations. In particular, the radiation damage in the maximum power point (P_{MPP}), short-circuit current (J_{SC}), open circuit voltage (V_{OC}), diffusion current (I_{01}), recombination current (I_{02}) and series resistance (R_s) have been researched using the D_d approach, the one-dimensional optical device simulator PC1D [12] and a homemade numerical code based on genetic algorithms.

2. Methods

2.1. Radiation damage model to space solar cells

For a comprehensive analytical model of radiation-induced degradation in GaAs sub-cells, the variation of effective minority-carrier lifetime and base carrier concentration should be considered.

In the first place, the decrease of the effective minority-carrier lifetime (τ_{eff}) in the base layer of the GaAs devices can be expressed by [13]:

$$1/\tau_{eff} = 1/\tau_R + 1/\tau_{NR} \quad (1)$$

where τ_R and τ_{NR} are the radiative and non-radiative recombination lifetime, respectively. On the one hand, the radiative recombination lifetime model is given by [14]:

$$1/\tau_R = B \cdot N \quad (2)$$

where B is the radiative recombination probability and N is the base carrier concentration; and on the other hand, the non-radiative recombination lifetime is evaluated using the following equation [15, 16]:

$$1/\tau_{NR} = \sum_i \sigma_i v_{th} N_{ri} = (1/\tau_\phi - 1/\tau_0) = K\phi \quad (3)$$

where σ_i is the capture cross section of the minority-carrier by radiation-induced *i*th recombination center, ν_{th} is the thermal velocity of the minority-carrier, N_{ri} is the concentration of *i*th recombination center, τ_0 and τ_ϕ are the minority-carrier lifetime before and after irradiation respectively, and ϕ is the accumulated fluence. This model can be explained by the introduction of radiation-induced recombination centers in the base layer of the GaAs structures, which tend to affect the solar cell performance.

In the second place, the carrier removal effect in the base layer of the GaAs devices caused by radiation-induced defects can be described by [17]:

$$\rho_\phi = \rho_0 \cdot \exp(-R_C \cdot \phi/\rho_0) \quad (4)$$

where ρ_0 and ρ_ϕ are the base doping concentration before and after irradiation, respectively, and R_C is the carrier removal rate.

Table 1. Structure of p^+ n GaAs solar cell used in this study.

Layer	Doping (cm^{-3})	Thickness (μm)
p^+ contact	1.00×10^{19}	0.18
AlGaAs window	2.00×10^{18}	0.03
p emitter	3.85×10^{17}	0.48
n base	3.40×10^{16}	2.85
n^+ buffer	3.12×10^{17}	0.54
n substrate	4.52×10^{18}	2.00

2.2. Simulation details

With the aim of validating the radiation damage model used in this work, numerical simulations of a $0.5 \times 0.5\,cm^2$ p^+ n GaAs solar cell with similar characteristics to that studied in reference [18], were performed in the PC1D simulator. In table 1 we give a complete description of the simulated device structure. Gaussian profiles for the doping distribution have been considered as an approximation to the real doping profiles. The use of the Gaussian function to approximate the real doping profiles is more appropriate than the use of the uniform or linearly graded models, because of the real distribution of dopant in the semiconductor substrate [19, 20].

In order to fit the electrical parameters (P_{MPP}, J_{SC} and V_{OC}) and the external quantum efficiency (*EQE*)

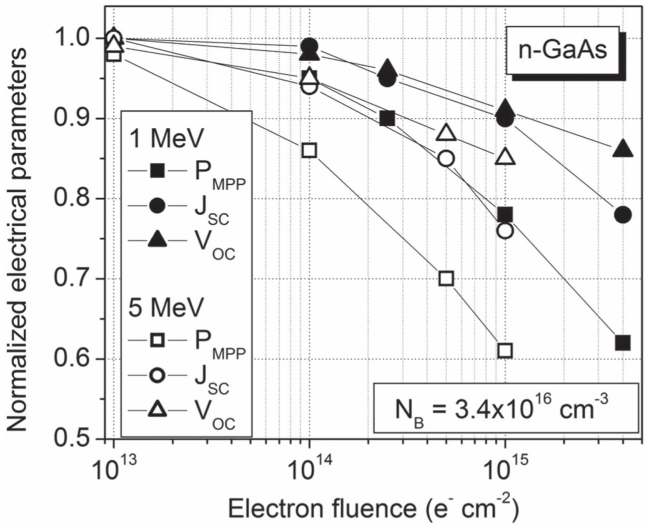

Figure 1. Normalized electrical parameters (P_{MPP}, J_{SC}, V_{OC}) as a function of fluence for 1 and 5 MeV electron on the n-GaAs solar cell described in table 1.

Table 2. Physical parameters used in the numerical analysis.

Physical parameters at 300 K	GaAs	AlGaAs
Electron mobility, μ_e($cm^2\,V^{-1}\,s^{-1}$)	8500	6250
Hole mobility, μ_h($cm^2\,V^{-1}\,s^{-1}$)	400	300
Dielectric constant	12.9	12.2
Band gap (eV)	1.424	1.817
Intrinsic carrier concentration, n_i (cm^{-3})	1.79×10^6	1750

to the experimental data without and with electron radiation, the following fitting parameters were used in the simulations: $B = 2.00 \times 10^{-10}\,cm^3\,s^{-1}$, $\tau_0 = 24$ ns, $K(1\,MeV) = 8.00 \times 10^{-13}\,cm^2\,s^{-1}$, $K(5\,MeV) = 3.00 \times 10^{-12}\,cm^2\,s^{-1}$, $R_C(1\,MeV) = 5\,cm^{-1}$ and $R_C(5\,MeV) = 10\,cm^{-1}$. Finally, a non-uniform front reflectance of the device was considered. Table 2 summarizes the other physical parameters used in the numerical analysis. The intrinsic carrier concentration for GaAs was extracted from [9]. The solar illumination conditions were AM0 spectrum, 1 sun and 25 °C. The mobility values shown in table 2 are for undoped materials. The PC1D software used in simulations includes the numerical models that take into account the variation in mobilities when the different layers are doped with n- or p-type impurities.

Figure 1 shows data obtained from simulation runs of the electrical parameters degradation (P_{MPP}, J_{SC}, V_{OC}) produced by increasing fluences of monoenergetic electrons with energies of 1 MeV (data with filled symbols) and 5 MeV (data with empty symbols). The values presented are normalized to those corresponding to the non-irradiated devices, which are ~18 mW cm^{-2}, ~23 mA cm^{-2} and ~0.95 V, for P_{MPP}, J_{SC} and V_{OC}, respectively. The lines through the data points are only intended to guide the eye.

These results agree very well with experimental values extracted from [18], such as can be observed in table 3 for non-normalized values. It can be seen in figure 1 that, for a given degradation level, the electron energy decreases when the fluence level is increased, indicating that the higher energy electrons lead to relatively more damage. However, degradations at different electron energies can be correlated using the D_d method, as is discussed below.

3. Results and discussion

3.1. Analysis of P_{MPP}, J_{SC} and V_{OC} for solar cells with different base doping concentration

The analysis of electron-induced damage by means of the D_d concept involves several steps, which have been extensively discussed in detail in previous publications [6, 18, 21]. In this method, the effective displacement damage dose ($D_{eff}(E)$) is used in place of the electron fluence ϕ. The $D_{eff}(E)$ parameter is defined for a reference energy level, which is usually taken as 1 MeV. The effective 1 MeV displacement damage dose $D_{eff}(1\,MeV)$ is defined by:

$$D_{eff}(1\,MeV) = D_d(E) \cdot \left(\frac{S(E)}{S(1\,MeV)}\right)^{(n-1)} \quad (5)$$

where $D_d(E)$ is the absorbed displacement damage dose, $S(E)$ is the appropriate NIEL value for electrons of energy E on the GaAs material, and the n-parameter is related to the nonlinear dependence of the electron damage coefficients on the NIEL. The $D_d(E)$ values are determined by multiplying the electron fluence ϕ by $S(E)$.

In this work, the D_d methodology has been applied to the same data set shown in figure 1 for the n-GaAs solar cell described in table 1. The exponent n was determined through a nonlinear least squares fitting of expression (5) at 1 and 5 MeV electron energy. Values of NIEL for GaAs used in this paper were 2.66×10^{-5} and $7.18 \times 10^{-5}\,MeV\,cm^2\,g^{-1}$ for 1 and 5 MeV electrons respectively [6]. Figure 2 shows the normalized data from figure 1 as a function of the effective 1 MeV displacement damage dose given by expression (5). The best values of n that cause the data of figure 2 seem to collapse well on a single characteristic curve for each electrical parameter are 1.30, 1.70 and 1.37, for P_{MPP}, J_{SC} and V_{OC}, respectively. The fit curves for the electrical parameters can also be observed in figure 2. These characteristic curves have been fitted using the semi-empirical expression to describe radiation-induced degradation of the maximum power point, short-circuit current and open circuit voltage given by [6]:

$$N(E) = 1 - C \cdot \log(1 + D_{eff}(E)/D_x) \quad (6)$$

where $N(E)$ represents the normalized parameter of interest: P_{MPP}, J_{SC}, or V_{OC}, after exposure to a given dose of electrons, whereas C and D_x are fitting parameters.

Table 4 contains the values of C, D_x and n for the characteristic curves presented in figure 2. In table 4 one can also observe that the values for the maximum power point are in good agreement with the fit values extracted from [18].

In order to fully understand the degradation in the P_{MPP}, J_{SC}, and V_{OC} caused by electrons of any energy, as a function of n-base carrier concentration (N_B), the D_d methodology was

Table 3. Values of P_{MPP}, J_{SC}, V_{OC} obtained from simulations and comparison with experimental data published in the literature.

		P_{MPP} (mW cm^{-2})		J_{SC}(mA cm^{-2})		V_{OC} (V)	
Energy (MeV)	Fluence (e$^-$ cm^{-2})	This work	Reference [18]	This work	Reference [18]	This work	Reference [18]
0	0	17.9	18.0	22.8	22.9	0.95	0.95
1	1.00×10^{13}	17.7	17.9	22.8	22.9	0.95	0.94
	1.00×10^{14}	17.0	16.9	22.6	22.2	0.93	0.92
	2.50×10^{14}	16.1	15.5	21.7	21.3	0.91	0.90
	1.00×10^{15}	14.0	14.1	20.5	20.2	0.86	0.88
	4.00×10^{15}	11.1	11.2	17.8	17.0	0.82	0.83
5	1.00×10^{13}	17.5	17.8	22.7	22.8	0.94	0.94
	1.00×10^{14}	15.4	15.7	21.4	21.3	0.90	0.91
	5.00×10^{14}	12.6	13.0	19.4	19.5	0.84	0.86
	1.00×10^{15}	10.9	10.8	17.3	17.2	0.81	0.82

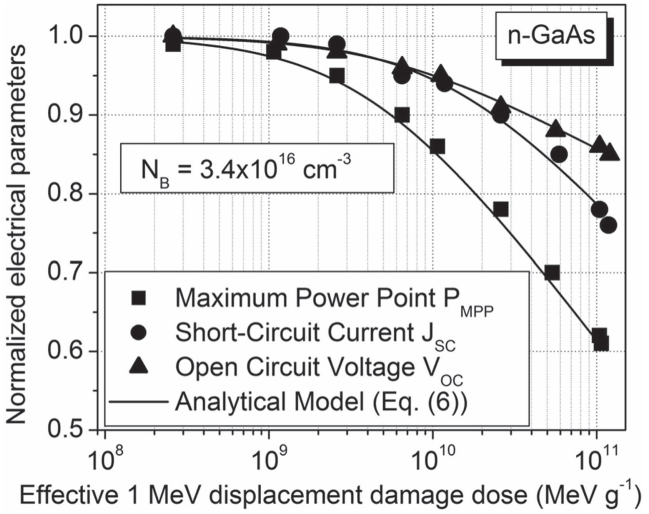

Figure 2. Normalized electrical parameters (P_{MPP}, J_{SC}, V_{OC}) as a function of effective 1 MeV electron absorbed displacement damage dose on the n-GaAs solar cell described in table 1. This is the same data set shown in figure 1. The solid lines represent the characteristic curves for each electrical parameter.

Table 4. Values of the fitting parameters for the electron irradiation data on the n-GaAs solar cell described in table 1 and comparison with the fit values published in the literature for P_{MPP}.

Electrical parameters		C	D_x (MeV g^{-1})	n
P_{MPP}	This work	0.28	4.35×10^9	1.30
P_{MPP}	Reference [18]	0.282	4.35×10^9	1.29
J_{SC}	This work	0.22	1.40×10^{10}	1.70
V_{OC}	This work	0.14	5.70×10^9	1.37

employed to nineteen different GaAs solar cells. Specifically, with regard to the simulated device structure presented in table 1, the n-base region was contaminated at nineteen different doping levels varied from 1.00×10^{15} to 1.00×10^{17} cm^{-3}. The other values of table 1 have remained unchanged.

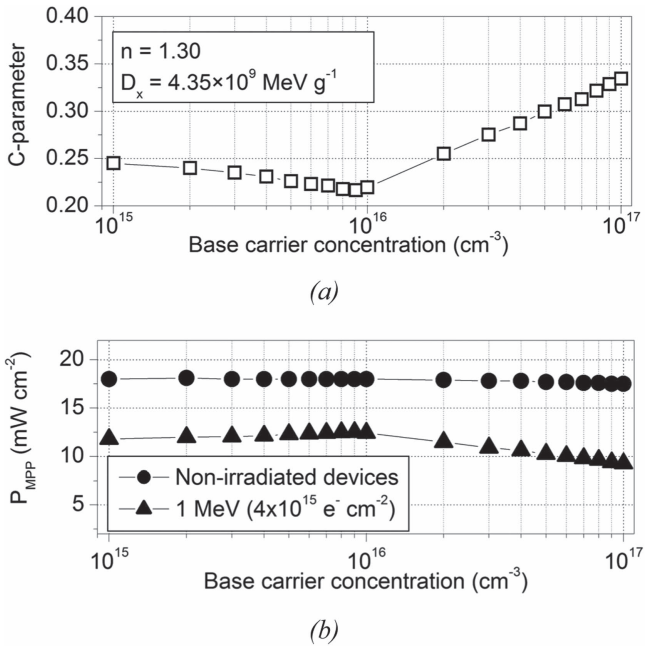

Figure 3. Base carrier concentration versus: (*a*) *C*-parameter from expression (6) for the maximum power point; (*b*) maximum power point for without and with electron radiation.

For each of the simulated devices the characteristic curves fitted by expressions (5) and (6) for P_{MPP}, J_{SC} and V_{OC} have been obtained. In all cases, no changes were obtained in the values of n for the entire range of N_B considered in this work. In contrast, if D_x values are kept fixed to those presented in table 4, then it has been found that the values of C from expression (6) suffer significant variations with N_B as is shown in figures 3(*a*)–5(*a*) for P_{MPP}, J_{SC} and V_{OC}, respectively. For the purpose of a better understanding of the variation of the *C*-parameter with respect to the n-base doping concentration, the data of P_{MPP}, J_{SC} and V_{OC} obtained from simulations for two extreme cases (without and with electron radiation), as a function of N_B, are presented in figures 3(*b*)–5(*b*), respectively. The lines drawn are only intended to guide the eye.

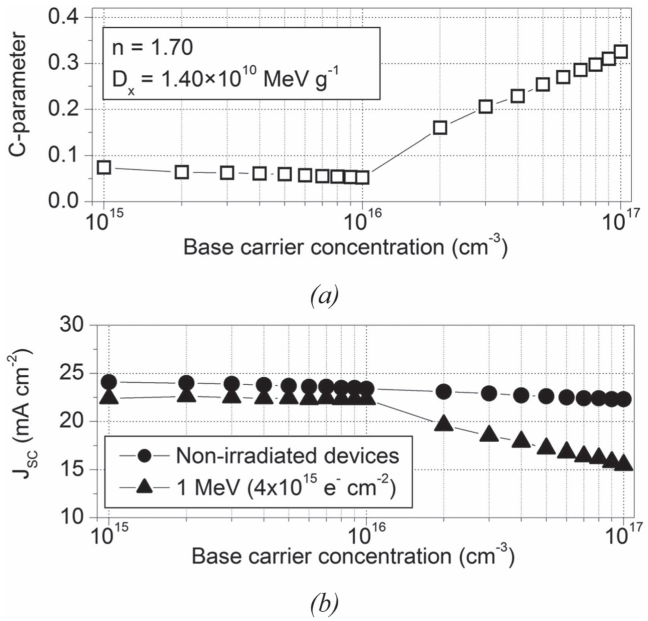

Figure 4. Base carrier concentration versus: (*a*) *C*-parameter from expression (6) for the short-circuit current; (*b*) short-circuit current for without and with electron radiation.

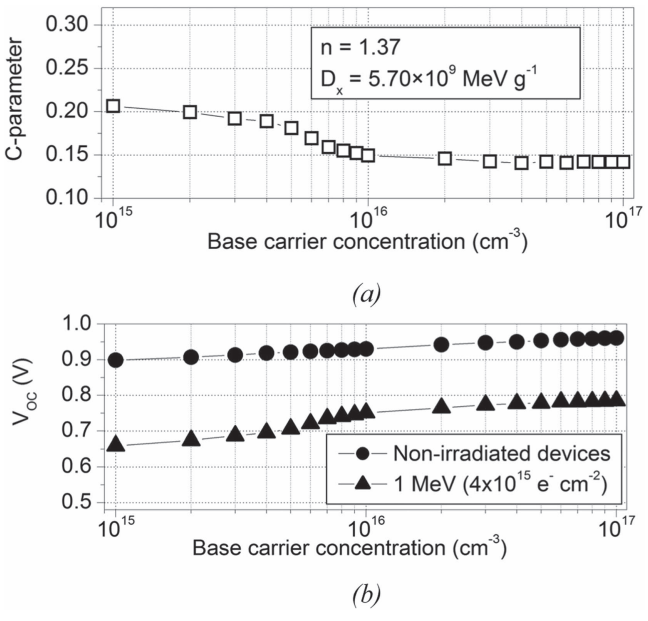

Figure 5. Base carrier concentration versus: (*a*) *C*-parameter from expression (6) for the open circuit voltage; (*b*) open circuit voltage for without and with electron radiation.

From expression (6), if the D_x value is considered fixed, the best condition to achieve the lesser degradation in the P_{MPP}, J_{SC}, and V_{OC} is obtained for lower values of C. It can be seen in figures 3(*a*) and (*b*) that there is an optimum value of N_B (close to $1 \times 10^{16}\,cm^{-3}$), for which the best radiation tolerance of P_{MPP} (that is, the minimum value of C) is obtained. For N_B above $1 \times 10^{16}\,cm^{-3}$, an abrupt increase in the C-parameter is observed when the base carrier concentration is increased, which tends to affect the solar cell performance. This behavior can be understood by a decrease of the radiative recombination lifetime and an increase in the radiation-induced recombination centers (and in consequence a decrease of the effective minority-carrier lifetime), according to expressions (1), (2) and (3). Finally, a gradual increase of the C value is observed for N_B below $1 \times 10^{16}\,cm^{-3}$, which can be attributed to the carrier removal effect in the base layer caused by radiation-induced defects. According to expression (4), the main influence of this effect is observed for the lowest N_B. A similar behavior to that described for P_{MPP} can also be observed in figures 4(*a*) and (*b*) for J_{SC}. In opposition, figures 5(*a*) and (*b*) show that the lesser degradation in the V_{OC} is obtained for N_B above $1 \times 10^{16}\,cm^{-3}$. The data presented in figures 3(*a*)–5(*a*) together with expressions (5) and (6), can be used to predict the radiation-induced degradation of P_{MPP}, J_{SC} and V_{OC} for both electron energy and a wide range of N_B.

3.2. Analysis of I_{01}, I_{02} and R_s by means of the D_d methodology

In order to study the behavior of a solar cell under different operating conditions, the most commonly used electrical equivalent circuit is the double diode model shown in figure 6 [22], where two diodes are connected in parallel to a light generated current source, I_{ph}.

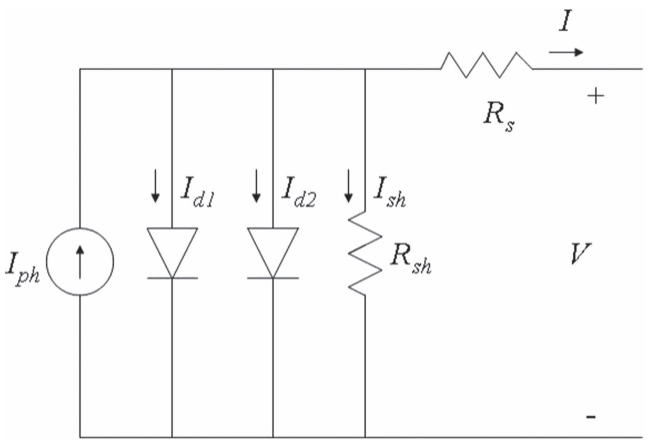

Figure 6. Two-diode equivalent circuit model of a solar cell.

The currents through the first and second diode, I_{d1} and I_{d2}, are currents due to diffusion in the quasi-neutral regions and recombination in the space-charge regions, respectively. R_s and R_{sh} are the series resistance and shunt resistance, respectively. The first one represents the resistance due to both contact resistances and movement of current through the emitter and base regions; and the second one represents the current leakage across the p-n junction of the solar cell. Finally, I and V are the output current and the output voltage of the solar cell respectively, which are related through the following equation [4, 22]:

$$\begin{aligned} I &= I_{ph} - I_{d1} - I_{d2} - I_{sh} = I_{ph} - I_{01} \\ &\times \left\{ \exp\left[\frac{q(V + IR_s)}{n_1 kT} \right] - 1 \right\} - I_{02} \\ &\times \left\{ \exp\left[\frac{q(V + IR_s)}{n_2 kT} \right] - 1 \right\} - \frac{V + IR_s}{R_{sh}} \end{aligned} \tag{7}$$

where I_{sh} is the shunt resistor current, I_{01} and I_{02} are the reverse saturation currents of diodes 1 and 2 respectively, n_1 and n_2 are the diffusion and recombination diode ideality factors respectively, q is the electronic charge, k is the Boltzmann's constant and T is the temperature in kelvin.

A numerical code based on genetic algorithms implemented in Matlab, fully developed by the authors, has been used in order to extract the parameters from expression (7), such as I_{ph}, I_{01}, I_{02}, R_s, R_{sh}, n_1 and n_2, of the same n-GaAs solar cell structure described in table 1, under illumination and electron-beam irradiation of 1 and 5 MeV. The genetic algorithms are computational models that mimic the biological evolution process for solving problems in a wide domain [23]. Starting from an initial population, in each stage the algorithm applies genetic operators in order to rank and select the best individuals. Each individual in the population is a possible solution to the problem. The current population of solutions produces the children for the next step of the algorithm by means of reproduction operators, namely crossover and mutation. Therefore, the initial population converges to the optimal solution after successive generations. The genetic algorithms have previously been used by other authors to extract the electrical parameters of solar cells [24, 25].

The implementation of genetic algorithms used in this work is based on the following considerations:

- Binary representation is used as a solution encoding.
- Fitness function based on equation (7), is expressed as

$$\begin{aligned} f(I_{ph}, I_{01}, I_{02}, R_s, R_{sh}, n_1, n_2) &= I_{ph} - I - I_{d1} - I_{d2} - I_{sh} \\ &= I_{ph} - I - I_{01}\left\{\exp\left[\frac{q(V+IR_s)}{n_1 kT}\right] - 1\right\} \\ &\quad - I_{02}\left\{\exp\left[\frac{q(V+IR_s)}{n_2 kT}\right] - 1\right\} - \frac{V+IR_s}{R_{sh}} \end{aligned} \tag{8}$$

The optimum solution is achieved when $f(I_{ph}, I_{01}, I_{02}, R_s, R_{sh}, n_1, n_2) = 0$.

- Random selection of the initial population.
- Initial population size: 200 individuals.
- Roulette wheel is used as selection criterion.
- The one-point crossover is employed with the crossover probability 0.75.
- Mutation probability 0.001.
- The genetic algorithm is executed 500 generations.

The input data for the genetic algorithms are a set of values of the *I–V* curves obtained from PC1D simulations for different electron fluences and energies. It is often assumed that $n_1 = 1$, $n_2 = 2$, and the light generated current, I_{ph} to be equal to the short-circuit current I_{SC} [4, 22, 25]. Additionally, the effect of radiations on the R_{sh} can be negligible [26]. Thus, the I_{01}, I_{02} and R_s parameters are the most strongly affected by the space radiation environment.

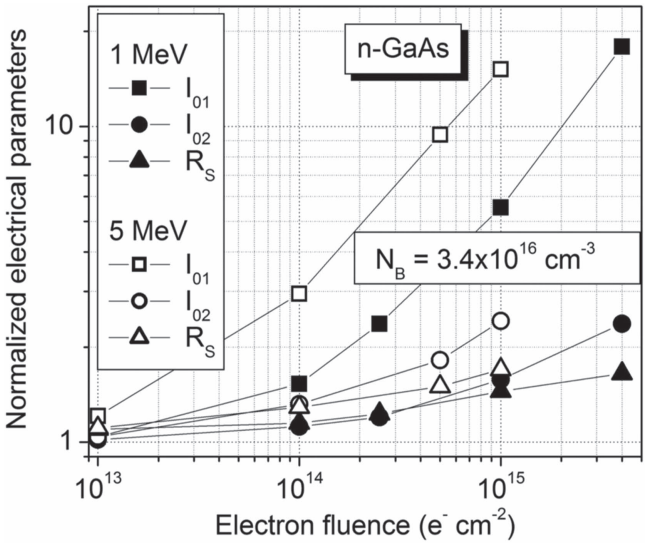

Figure 7. Normalized electrical parameters (I_{01}, I_{02}, R_s) as a function of fluence for 1 and 5 MeV electron on the n-GaAs solar cell described in table 1.

Results obtained on the degradation of I_{01}, I_{02} and R_s after electron irradiation are shown in figure 7, for the solar cell detailed in table 1. The filled and empty symbols correspond to the values obtained for electrons with energies of 1 and 5 MeV respectively. The lines through the data points are only intended to guide the eye. These values are presented as normalized with respect to those corresponding to the non-irradiated devices, which are $\sim 7.2 \times 10^{-11}$ A, $\sim 3.4 \times 10^{-6}$ A and $\sim 1.6\,\Omega$, for I_{01}, I_{02} and R_s, respectively. These non-normalized values are consistent with literature data since I_{02} is generally 3 to 7 orders of magnitude larger than I_{01} [22].

It can be seen that an abrupt increase (close to 18 times) in diffusion current and a gradual increase of recombination current (close to 2.4 times) and series resistance (close to 1.7 times) are observed for fluence irradiation below $4.00 \times 10^{15}\,e^-\,m^{-2}$. This significant change of I_{01}, considerably larger than the change in I_{02}, has also been reported previously in reference [22]. These effects can lead to severe failure of the solar cell.

It is also possible to observe in figure 7 that if the electron fluence is increased then the electron energy decreases for a given degradation level, indicating that the higher energy electrons lead to relatively more damage. Therefore, the displacement damage dose (D_d) method has been applied in order to collapse into single characteristic curves for each electrical parameter (the same data set shown in figure 7), as can be seen in figure 8. The best values of n from expression (5) obtained through a nonlinear least squares fitting at 1 and 5 MeV electron energy were 1.22; 1.39 and 1.41 for I_{01}, I_{02} and R_s, respectively.

The fit of the data set corresponding to each electrical parameter considered can also be observed in figure 8. These characteristic curves have been obtained from a logistic sigmoid fit using the programming language Python [27] and can

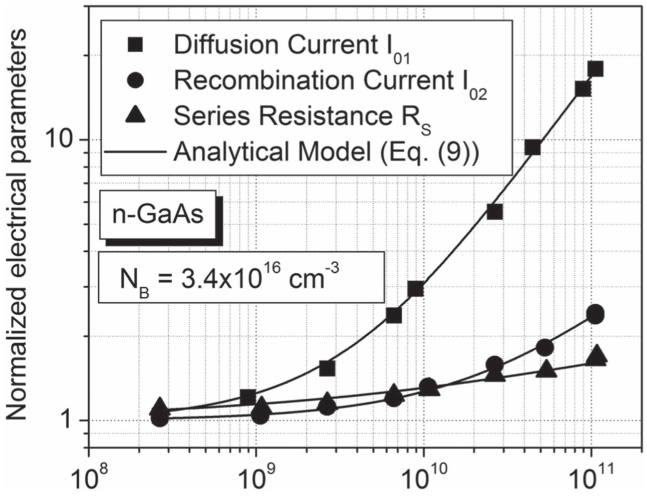

Figure 8. Normalized electrical parameters (I_{01}, I_{02}, R_s) as a function of effective 1 MeV electron absorbed displacement damage dose on the n-GaAs solar cell described in table 1. This is the same data set shown in figure 7. The solid lines represent the characteristic curves for each electrical parameter.

Table 5. Values of fitting parameters for the electron irradiation data on the n-GaAs solar cell described in table 1.

Electrical parameters	C	D_x (MeV g^{-1})	p	n
I_{01}	150	1.00×10^{12}	0.94	1.22
I_{02}	10	1.00×10^{12}	0.77	1.39
R_s	3	1.00×10^{12}	0.38	1.41

be expressed by:

$$M(E) = \frac{1 - C}{1 + (D_{\text{eff}}(E)/D_x)^p} + C \qquad (9)$$

where $M(E)$ represents the normalized parameter of interest: I_{01}, I_{02} and R_s after exposure to a given dose of electrons, whereas C, D_x and p are fitting parameters. The C-parameter in equation (9) represents the theoretical limit value of $M(E)$ that would be obtained if $D_{\text{eff}}(E)$ becomes much greater than D_x. Table 5 contains the values of C, D_x, p and n for the characteristic curves presented in figure 8. Expression (9) is useful to determine the radiation-induced degradation of the diffusion current, recombination current and series resistance for any electron energy.

4. Conclusion

The effects of electron irradiation on n-type GaAs sub-cells for InGaP/GaAs/Ge 3J solar cells have been studied through computer simulation. The displacement damage dose methodology together with the one-dimensional optical device simulator PC1D and a home-made numerical code based on genetic algorithms have been employed to analyze in detail the radiation response of the electrical parameters of all the simulated devices. The reduction of the effective minority-carrier lifetime and the carrier removal effect have been considered for the radiation damage model. The results obtained in this work show how the performance degradation of the maximum power point, short-circuit current and open circuit voltage, for a large range of electron energies, is a function of one of the design parameters, such as the n-base carrier concentration. In addition, an analytical model that relates the effective 1 MeV displacement damage dose with the diffusion current, recombination current and series resistance has been proposed to determine the radiation-induced degradation of these electrical parameters for any electron energy. These results are useful to contribute to the design of radiation-hardened devices and to enhance on-orbit expected mission lifetime.

Acknowledgments

This work was partially supported by the Universidad Nacional de La Plata, Argentina, by the Universidad Nacional Arturo Jauretche, Argentina, by the Universidad Nacional de Quilmes, Argentina and by the National Council Research (CONICET), Argentina.

References

[1] Xin G *et al* 2014 Performance evaluation and prediction of single-junction and triple-junction GaAs solar cells induced by electron and proton irradiations *IEEE Trans. Nucl. Sci.* **61** 1838–42
[2] Simic B *et al* 2013 Damage induced by neutron radiation on output characteristics of solar cells, photodiodes, and phototransistors *Int. J. Photoenergy* **2013** 582819
[3] Zhang X, Hu J, Wu Y and Lu F 2010 Impedance spectroscopy characterization of proton-irradiated GaInP/GaAs/Ge triple-junction solar cells *Semicond. Sci. Technol.* **25** 035007
[4] Anspaugh B E 1996 *GaAs Solar Cell Radiation Handbook* (Pasadena, CA: JPL Publication)
[5] Alurralde M 2004 Method using the primary knock-on atom spectrum to characterize electrical degradation of monocrystalline silicon solar cells by space protons *J. Appl. Phys.* **95** 3391–6
[6] Summers G P *et al* 1994 A new approach to damage prediction for solar cells exposed to different radiations *IEEE Proc. 1st World Conf. on Photovoltaic Energy Conversion* pp 2068–75
[7] Stassinopoulos E G and Raymond J P 1988 The space radiation environment for electronics *Proc. IEEE* **76** 1423–42
[8] Cappelletti M A *et al* 2013 Theoretical study of the maximum power point of n-type and p-type crystalline silicon space solar cells *Semicond. Sci. Technol.* **28** 045010
[9] Sato S *et al* 2009 Degradation modeling of InGaP/GaAs/Ge triple-junction solar cells irradiated with various-energy protons *Sol. Energy Mater. Sol. Cells* **93** 768–73
[10] Rong W, Yunhong L and Xufang S 2008 Effects of 0.28–2.80 MeV proton irradiation on GaInP/GaAs/Ge triple-junction solar cells for space use *Nucl. Instrum. Methods Phys. Res., Sect.* B **266** 745–9
[11] Sumita T *et al* 2003 Proton radiation analysis of multi-junction space solar cells *Nucl. Instr. and Meth. Phys. Res.* B **206** 448–51

[12] PC1D available online at (http://engineering.unsw.edu.au/energy-engineering/pc1d-software-for-modelling-a-solar-cell)
[13] Sermage B *et al* 1989 Radiative and non-radiative recombination in GaAs/$Al_xGa_{1-x}As$ quantum wells *Superlattices Microstruct.* **6** 373–6
[14] Hooft G W *et al* 1985 Temperature dependence of the radiative recombination coefficient in GaAs—(Al, Ga)As quantum wells *Superlattices Microstruct.* **1** 307–10
[15] Loferski J J and Rappaport P 1958 Radiation damage in Ge and Si detected by carrier lifetime changes: damage thresholds *Phys. Rev.* **111** 432–9
[16] Morita Y *et al* 1997 Anomalous degradation in silicon solar cells subjected to high-fluence proton and electron irradiations *J. Appl. Phys.* **81** 6491–3
[17] Khan A *et al* 2002 Thermal annealing study of 1 MeV electron-irradiation-induced defects in n + p InGaP diodes and solar cells *J. Appl. Phys.* **91** 2391–7
[18] Warner J H *et al* 2006 Correlation of electron radiation induced-damage in GaAs solar cells *IEEE Trans. Nucl. Sci.* **53** 1988–94
[19] Schumacher J O 2000 Numerical simulation of silicon solar cells with novel cell structures *PhD Thesis* Freiburg, Germany
[20] Rinaldi N 2000 Analysis of the depletion layer of exponentially graded P–N junctions with nonuniformly doped substrates *IEEE Trans. Electron Devices* **47** 2340–6
[21] Ming L *et al* 2013 Displacement damage dose approach to predict performance degradation of on-orbit GaInP/GaAs/Ge solar cells *Nucl. Instr. and Meth. Phys. Res.* B **307** 362–5
[22] Wolf M *et al* 1977 Investigation of the double exponential in the current-voltage characteristics of silicon solar cells *IEEE Trans. Electron Devices* **24** 419–28
[23] Davis L 1991 *Handbook of Genetic Algorithms* (New York: Van Nostrand Reinhold)
[24] Jervase J A *et al* 2001 Solar cell parameter extraction using genetic algorithms *Meas. Sci. Technol.* **12** 1922–5
[25] Appelbaum J and Peled A 2014 Parameters extraction of solar cells—a comparative examination of three methods *Sol. Energy Mater. Sol. Cells* **122** 164–73
[26] Hu Z, He S and Yang D 2004 Effect of <200 keV proton radiation on electric properties of silicon solar cells at 77 K *Nucl. Instr. and Meth. Phys. Res.* B **217** 321–6
[27] Python available online at (https://python.org)